DOI: https://doi.org/10.54966/jreen.v29i2.1847

Journal of Renewable Energies

Revue des Energies Renouvelables

Journal home page: https://revue.cder.dz/index.php/rer

Conference paper

Modeling of VAWT-AFPMSG using the finite element method for wind energy conversion

Lina Bouhafs [a,*], **Salah Tamalouzt** [a], **Ahcene Bouzida** [b], **Mustafa Ergin Şahin** [c]

[a] *Laboratory of Industrial Technology and Information (LTII), Faculty of Technology, University of Bejaia, 06000 Bejaia, Algeria*

[b] *Faculty of Applied Sciences, Ali Mohand Oulhadj University, 10000 Bouira, Algeria*

[c] *Department of Electrical and Electronics Engineering, RTE University, 53100, Rize, Türkiye*

ARTICLE INFO

Article history:
Received December 12, 2025
Revised April 27, 2026
Accepted April 27, 2026
Available online April 28, 2026
Published May 4, 2026

Keywords:
Axial flux machine,
Permanent magnet generator,
Vertical axis wind turbine,
Finite element analysis,
Field-oriented control.

ABSTRACT

In the context of the global energy transition and decarbonization efforts, wind energy has become a crucial component of sustainable power generation. Among the various electrical generators utilized, the Axial Flux Permanent Magnet Synchronous Generator has garnered considerable attention due to its significant advantages in wind energy conversion. Its axial configuration is particularly advantageous for applications where space and weight are critical factors. This article presents a detailed modeling and simulation of a vertical axis wind turbine system based on the Axial Flux Permanent Magnet Synchronous Generator. The design process began with the development of a 3D electromagnetic model in ANSYS Maxwell through RMxprt model, where both geometric and magnetic characteristics were defined. In parallel, MATLAB/Simulink was employed to model the wind turbine and implement a Maximum Power Point Tracking algorithm to maximize energy capture and field-oriented control. A co-simulation in Twin Builder integrating Maxwell and Simulink was developed to ensure realistic performance evaluation, enabling dynamic interaction between mechanical and electrical subsystems. This approach provided an effective platform for evaluating system performance in conjunction with the electromagnetic modeling of power electronic circuits.

1. INTRODUCTION

The global transition to renewable energy systems is crucial for combating climate change and sustainable energy supply. Among renewable technologies, wind energy plays a pivotal role because it

* *Corresponding author, E-mail address: lina.bouhafs@univ-bejaia.dz*

ISSN: 1112-2242 / EISSN: 2716-8247

Selection and peer-review under responsibility of the Technical Committee of the 3rd Electrical Engineering International Conference (EEIC'25)

is a clean, abundant, and inexhaustible resource(Adelekan et al., 2024; Burton et al., 2011; Zhu et al., 2023) . However, modern wind turbines face significant challenges related to efficiency, weight, and operational reliability, particularly in offshore environments, where harsh conditions necessitate robust yet lightweight designs (Bouhafs et al., 2025; Boztaş et al., 2021; Veers et al., 2023). Overcoming these limits demands rethinking wind capture and energy conversion. In this scop, the Axial Flux Permanent Magnet Synchronous Generator (AFPMSG) emerges as an innovative solution (Barmpatza, 2023). Unlike conventional radial flux generators (Ashrafzadeh et al., 2024), the AFPMSG features a compact, disc-shaped architecture that allows magnetic flux to circulate parallel to the rotational axis, enabling direct coupling with turbine blades. This design not only enhances torque density but also aligns seamlessly with low-speed wind regimes, maximizing energy yield under variable conditions (Çabuk & Üstün, 2023; de Azevedo & Barros, 2021).

The electromagnetic performance of the generator was examined using Finite Element Analysis (FEA) to support the design optimization process. FEA offers significant advantages by enabling precise modelling of electromagnetic, thermal, and electrical phenomena while considering non-linear material properties, magnetic saturation, and complex geometrical effects. Consequently, it is particularly effective in capturing fault-induced signatures that are often ignored by conventional analytical models. Moreover, FEA enables a comprehensive analysis of critical performance indicators, including electromagnetic torque, flux density distribution, induced back-EMF, losses, and efficiency, under variable operating conditions. In recent years, extensive research has adopted FEA-based modeling using ANSYS software for the design, optimization, and fault diagnosis of synchronous machines.

In recent years, several studies (Ahmadi et al., 2012; Esenboğa, 2024; Lakshmi et al., 2025) have focused on the electromagnetic simulation of wind energy conversion systems by integrating aerodynamic, mechanical, electrical, and control subsystems to achieve accurate and realistic modelling.

In (Esenboğa, 2024), the authors investigate the electromagnetic performance of PMSGs for wind turbine applications using the finite element method implemented in ANSYS Maxwell. A comparative analysis is conducted by considering different core materials, highlighting their impact on flux distribution, losses, efficiency, and overall generator performance. In (Mersha & Du, 2021), a co-simulation methodology is proposed for PMSM modelling by coupling ANSYS tools (Maxwell and Twin Builder) with MATLAB/Simulink. This approach aims to improve both the accuracy of motor design and the performance of control systems. In (Hölsch et al., 2024), a co-simulation methodology is introduced that combines models of motors, power electronics, and control systems to assess the behaviour of electric drives. This methodology allows for the analysis of optimized switching strategies without the need for experimental testing, particularly in electric vehicle applications.

In contrast, the present work focuses on axial flux permanent magnet synchronous generators (AFPMSGs), which offer superior performance and compactness, making them highly suitable for renewable energy conversion systems. Based on the relevance of co-simulation approach highlighted in previous works, this paper proposes an advanced co-simulation platform that combine MATLAB/Simulink with electromagnetic solvers to analyse the dynamic behaviour of the AFPMSG based wind turbines (WT-AFPMSG) under realistic operating conditions, as well as to implement the control of the WT-AFPMSG conversion system using field-oriented control (FOC).

In this study, a WT-AFPMSG system is modelled using FEA to evaluate the performance of the generator. The AFPMSG is designed in ANSYS Maxwell 3D through FEA, and its behaviour is further analysed via co-simulation with the power electronic interface in the Twin Builder environment. At the same time, the wind turbine is modelled in MATLAB/Simulink with an MPPT control strategy, and the FOC is applied to the generator to ensure effective regulation of flux and torque. Finally, a bidirectional co-simulation between Twin Builder and Simulink providing an accurate representation of the complete

system dynamics. First, the system was operated under constant speed conditions to evaluate and validate the performance of the system. Subsequently, a more realistic scenario was simulated by introducing variable speed operation, thereby reflecting the dynamic nature of wind energy conversion.

2. PRESENTED MODEL

The AFPMSG uses permanent magnets for excitation and is part of the axial flux family, where the magnetic flux flows parallel to the rotation axis. Compared to radial flux designs, axial flux machines offer high torque density, compact size, and high efficiency, making them ideal for vertical-axis wind turbines (Liu et al., 2025). Various configurations, single or dual rotors and stators are chosen according to application requirements.

2.1 Wind turbine design

In this study, A MATLAB/Simulink model with the field-oriented control (FOC) is developed to enhance wind turbine dynamics, robustness, and efficiency (Tabassum et al., 2024). A double closed-loop PI control system is used to stabilize the generator currents.

The variation of the wind speed is described by the following Eq. (1):

$$V = 7.5 + 0.035\sin(\frac{2\pi}{9}t) + 0.525\sin(\frac{2\pi}{3}t) + 0.35\sin(\frac{8\pi}{3}t) + 0.0875\sin(\frac{10\pi}{3}t) \quad (1)$$

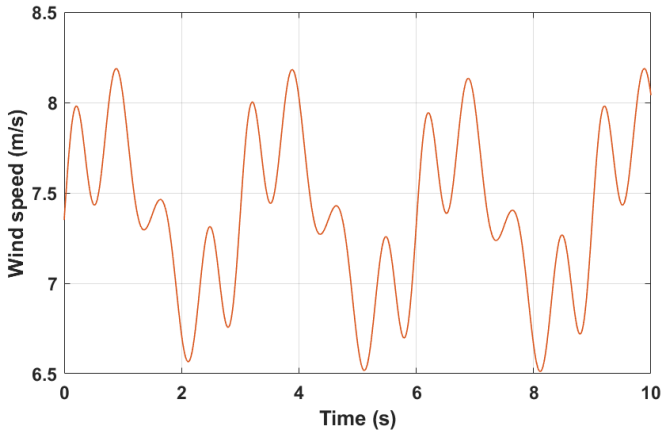

Fig 1. Wind speed profile

The shaft power produced at the turbine shaft is represented by Eq. (2) (Şahin et al., 2012):

$$P_t = \frac{1}{2}.C_p(\lambda,\beta).\rho.S.V_v^3 \quad (2)$$

2.1.1 Gearbox model

The gearbox is a device designed to increase the relatively low turbine speed Ω_t by a multiplication factor so as to match the higher generator shaft speed Ω_m , as expressed in Eqs. (3) and (4).

$$T_g = \frac{T_t}{G} \tag{3}$$

$$\Omega_t = \frac{\Omega_m}{G} \tag{4}$$

2.1.2 Model of the mechanical shaft

The fundamental dynamics of the wind turbine are described by the following simple mathematical model in Eqs. (5) and (6):

$$T_{total} = J \frac{d\Omega_m}{dt} \tag{5}$$

$$T_{total} = T_g - T_{em} - T_f \tag{6}$$

Consequently, the following Eq. (7) is obtained:

$$T_g - T_{em} = J \frac{d\Omega_m}{dt} + f\Omega_m \tag{7}$$

2.1.3 Maximum Power Point Tracking (MPPT) algorithm control

The MPPT strategy maximizes wind turbine power through controlling electromagnetic torque to keep the optimal speed ratio, as defined in Eq. (8) (Narimene et al., 2022):

$$T_{em-ref} = \frac{1}{2}.C_{p-\max} \frac{\rho.\pi.R^5}{G^3.\lambda_{optm}^3}.\Omega_m{}^2 \tag{8}$$

2.2 Field-oriented control

Field-oriented control (FOC) linearizes the AFPMSG by converting it into an equivalent DC machine, enabling decoupled control and improved dynamic performance (Farhan et al., 2021). the simulation diagram for the control applied to the AFPMSG system. This system includes a wind turbine that generates the electromagnetic torque reference $T_{em\text{-}ref}$, and establishes the current reference $I_{q\text{-}ref}$. The direct current reference $I_{d\text{-}ref}$ is set to zero, which reduces losses. These currents references are individually compared with the measured machine currents i_a, i_b and i_c after applying park transformation. The resulting errors are then fed into the conventional PI type regulators. A decoupling block generates the reference voltages $V_{d\text{-}ref}$ and $V_{q\text{-}ref}$. The outputs from the decoupling are then transformed from two phases to three-phase, producing the three reference voltages.

2.2.1 Decupling

The voltages depend on both the d and q axis currents, so decoupling is required. This decoupling is based on the introduction of compensating terms, as expressed in Eq. (9):

$$\begin{cases} e_d = \Omega_m L_q i_q \\ e_q = \Omega_m (L_d i_d + \phi_f) \end{cases} \tag{9}$$

Therefore, the mono-variable voltage equations are presented in Eq. (10) as follow:

$$\begin{cases} V_{d-ref} = V_d^{'} - e_d \\ V_{q-ref} = V_q^{'} + e_q \end{cases} \tag{10}$$

2.2.2 Synthesis of regulators

In this section, we introduce the transfer function of the PI controller is introduced, expressed in Eq. (11):

$$G(p) = K_p + \frac{K_i}{p} \tag{11}$$

The expressions derive from the machine's electrical parameters, that is, for I_d and I_q currents regulator (see Eqs. (12) and (13)).

$$\begin{cases} K_{pd} = \dfrac{3L_d}{\tau_d} \\ K_{id} = \dfrac{3R_s}{\tau_d} \\ \tau_d = \dfrac{L_d}{R_s} \end{cases} \tag{12}$$

$$\begin{cases} K_{pq} = \dfrac{3L_q}{\tau_q} \\ K_{iq} = \dfrac{3R_s}{\tau_q} \\ \tau_q = \dfrac{L_q}{R_s} \end{cases} \tag{13}$$

2.3 Axial flux permanent magnet generator design

The analysis of electromagnetic systems is fundamentally grounded in Maxwell's equations. This analysis relies on the simultaneous solution of the time-dependent Maxwell equations and the electrical equations governing the windings. Faraday-Maxwell's law (see Eq. 14) describes the electromagnetic induction resulting from time-varying flux, while Ampère-Maxwell's law (see Eq. 15) defines the relationship between the magnetic field, conduction currents, and displacement currents. By combining

these equations, we can determine the magnetic field distribution within the studied domain at any given moment.

$$\nabla \times E = -\frac{\partial B}{\partial t} \tag{14}$$

$$\nabla \times H = J + \frac{\partial D}{\partial t} \tag{15}$$

Equation 16 defines the expression employed to estimate the stator flux vector in the generator:

$$\nabla \times (\frac{1}{\mu} \nabla \times A) + \sigma \frac{\partial A}{\partial t} = J_{source} \tag{16}$$

In this study, the AFPMSG is initially conceptualized using an analytical model characterized by a single rotor and a single stator. Subsequently, the chosen configuration, which consists of 18 coils and 8 poles, is implemented in the Ansys Software to develop the FEA. The AFPMSG was initially designed within the RMxprt interface utilizing its rapid implementation capabilities for generator design and performance assessment. The specific parameters essential for the optimal performance of the generator are given in Table 1 and 2. then, the model was transformed into 3D representation, as illustrated in Fig. 2.

Table 1. Electrical Characteristics of the AFPMSG

Parameter	Value
Rated output power	550 W
Rated voltage	220 V
Rated speed	1500 rpm
Rated frequency	60 Hz
Coupling	Star
Resistance	36.33 ohm
Inductance	0.00625 H

Table 2. Geometrical Characteristics of the AFPMSG

Parameter	Value
Stator inner diameter	550 W
Stator puter diameter	220 V
Length of the stator core	1500 rpm
Rotor inner diameter	60 Hz
Rotor outer diameter	Star
Length of the rotor core	36.33 ohm
Air gap	0.00625 H
Magnet length	25 mm
Magnet thickness	8 mm

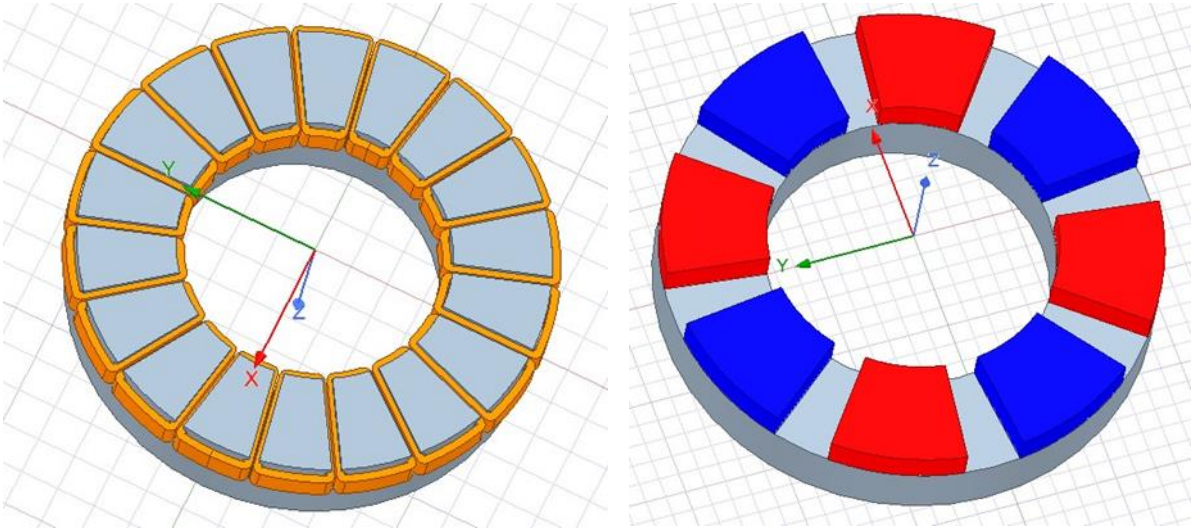

(a) (b)

Fig 2. Design of the AFPMSG in Maxwell 3D: (a) Stator part, (b) Rotor part

The electromagnetic equivalent circuit of the generator, designed using FEA software, can be coupled with the power electronics circuit using Twin Builder and MATLAB for co-simulation. This co-simulation connects the ANSYS and MATLAB software environments, allowing for data flow and system control between them.

3. SIMULATION AND RESULTS

The simulations are carried out over a duration of 500 ms using a time step of 10 µs. The wind turbine operates at a constant speed of 1500 rpm, while the generator supplies a fixed resistive load.

Figure 3 illustrates the magnetic field distribution in the AFPMSG, depicting the overall field throughout the generator while emphasizing the regions inside the magnets and stator slots. A significant flux density is visible at the stator teeth and magnets, reflecting the efficient magnetic behaviour of the system.

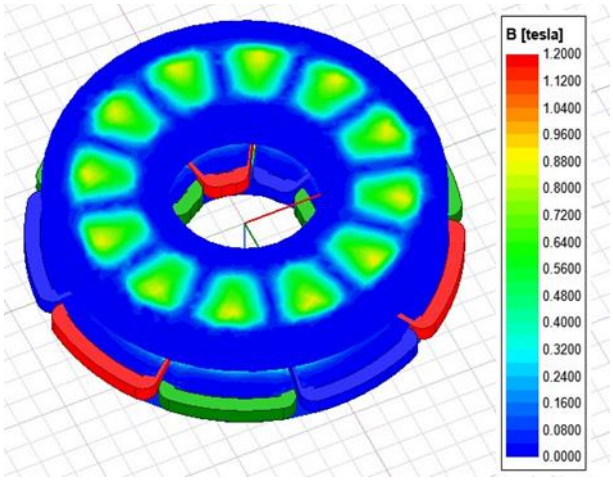

Fig 3. Magnetic field distribution in the AFPMSG

A no-load test of the VAWT-AFPMSG is carried out from 0 to 60 ms, after which a balanced three-phase resistive load is suddenly connected to the generator. Based on data from the validated FEA model, Figs. 4, 5, and 6 show the stator voltage waveform, line current, and electromagnetic torque when the rotor operates at a constant speed. Fig. 4 demonstrates that under no-load conditions, the voltage maintains its nominal amplitude; however, immediately after the load connection, there is a small decline is observed due to voltage regulation effects resulting from the increased current demand. This voltage alteration is accompanied, as illustrated in Fig. 5, by a rapid increase in the three-phase line currents, which were nearly zero before the application of the load, indicating the absence of active power generation. Following the load connection, the currents rise rapidly to meet the power demand while preserving a balanced sinusoidal waveform. Fig. 6 reveals that the electromagnetic torque, which is minimal under no-load conditions increases significantly once the load is applied, thereby providing the requisite mechanical power for electrical generation. The transient oscillations observed immediately following the load connection are attributed to the sudden change in operating conditions, after which the system rapidly stabilizes to a steady state.

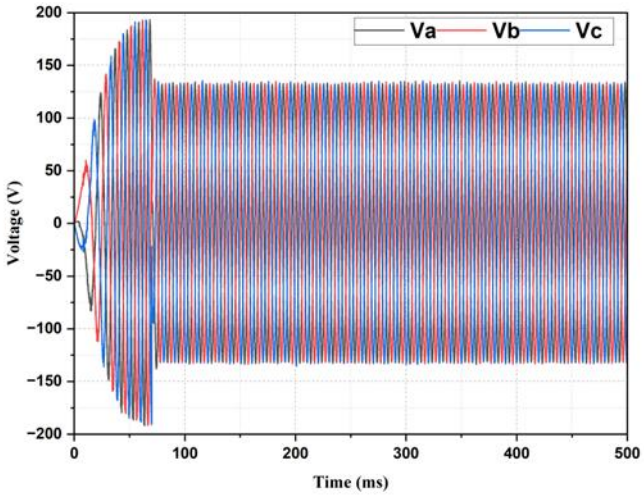

Fig 4. Transient voltage response of the VAWT-AFPMSG system

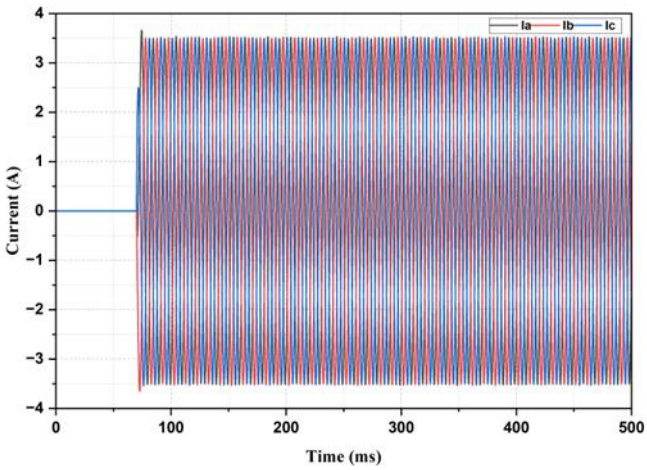

Fig 5. Transient current response of the VAWT-AFPMSG system

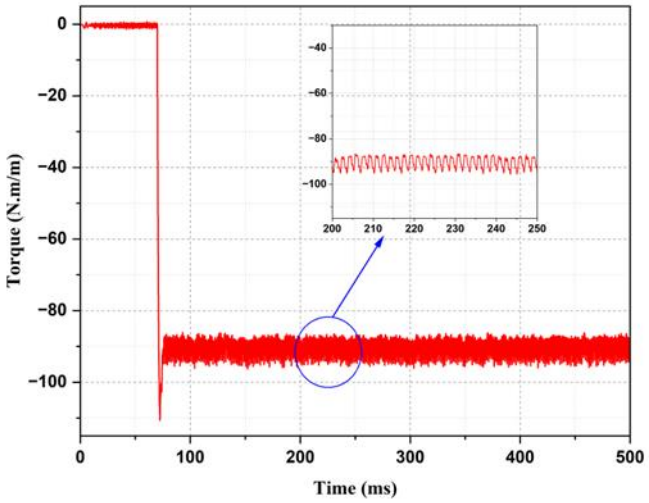

Fig 6. Transient torque response of the VAWT-AFPMSG system

Figures. 7 and 8 show the current and voltage responses, confirming that both quantities increase progressively as the wind turbine speed increases. This behaviour is expected since, in AFPMSG, the induced electromotive force (EMF) increases, and therefore the produced voltage varies with the rotational speed. As a result, the current also increases with speed. When the turbine spins faster, the generator produces a higher voltage, which results in a higher output current, provided the electrical load stays constant. These results confirm that the generator behaves correctly under variable-speed conditions**.**

The simulation results, depicted in Fig. 9, show the torque waveform of the generator, which operates in three distinct steady states that correspond to various rotational speeds. In the first phase (0–80 s), the torque decreases rapidly before stabilizing at an average of approximately 70 Nm, accompanied by moderate oscillations. From 200 s to 350 s, a further increase in torque is observed, stabilizing around 90 Nm. After 350 s, the torque reaches its highest average value of about 100 Nm. In these regions, the torque displays periodic ripple characteristics. Notably, the ripple amplitude increases slightly in the third region, suggesting a more dynamic mechanical or electrical interaction. Despite these transitions, the torque remains stable, confirming the effective power generation behaviour of the AFPMSG under increasing speed conditions with a constant resistive load.

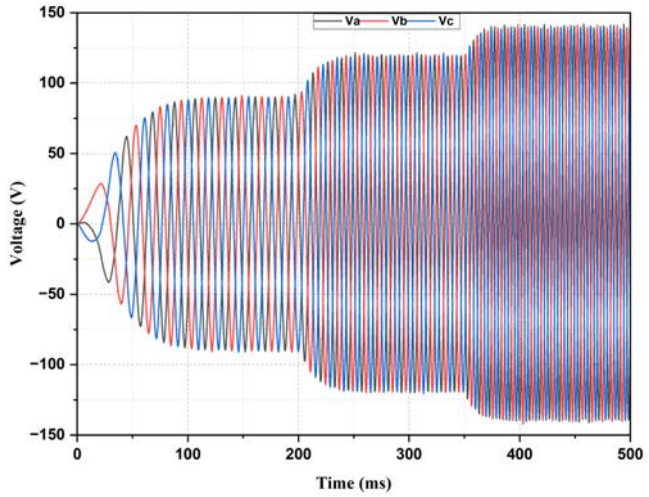

Fig 7. Three-phase voltage waveforms under variable speed condition

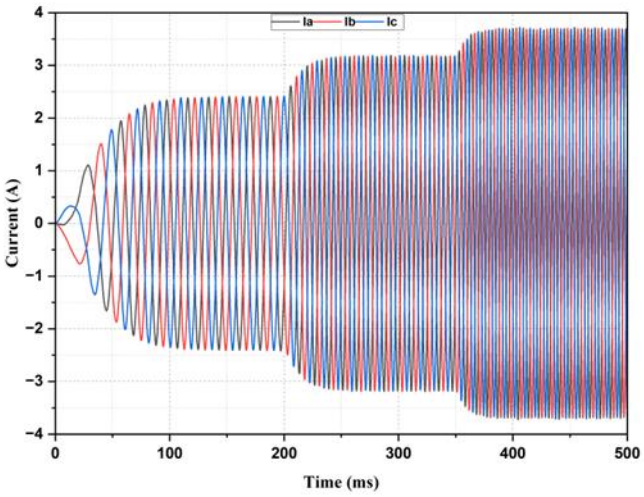

Fig 8. Three-phase current waveforms under variable speed condition

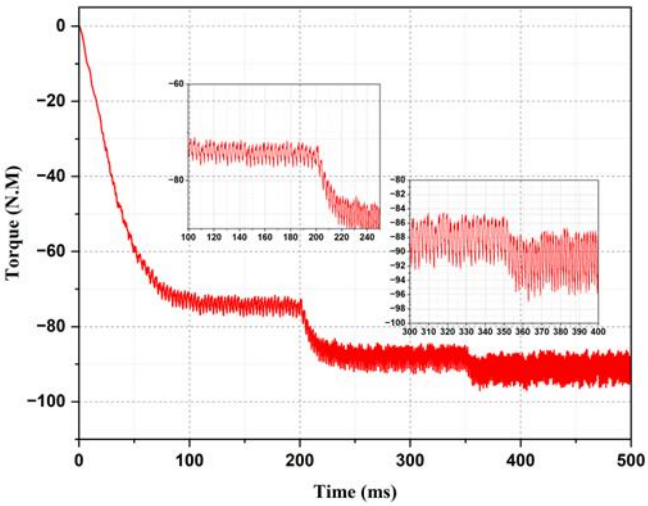

Fig 9. Electromagnetic torque under variable speed condition

4. CONCLUSION

The design and regulation system of the VAWT-AFPMSG was developed using numerical analysis. First, a 3D electromagnetic model of the AFPMSG was created through the RMxprt tool, which established a structural representation based on the necessary size and parameters for FEA. Next, MATLAB/Simulink was employed to model the VAWT and simulate the AFPMSG's control system, including direct vector control. A co-simulation model was then constructed in both Ansys and MATLAB/Simulink. For the co-simulation to operate efficiently, continuous data transfer among the individual component models is essential. This integrated process has effectively developed a reliable and high-performance AFPMSG, ensuring that all design criteria and performance indicators are met. The co-simulation methodology, which combines MATLAB/Simulink capabilities with Ansys interfaces, has been crucial in achieving a more realistic representation of the physical system. This approach not only enhances result accuracy but also provides a deeper understanding of the machine's behavior under real operating conditions, highlighting the importance of co-simulation in the design and evaluation of advanced energy systems.

NOMENCLATURE

C_p	Power coefficient
$C_{p\text{-}max}$	Maximum power coefficient
D	Electric flux density
E	Electric field
G	Factor of multiplication
H	Magnetic field
i_d,i_q	Park components of currents along the *dq* axes
V_d,V_q	Park components of voltages along the *dq* axes
J	Conduction current density
J_t	Total inertia
L_d,L_q	Park components of inductances along the *dq* axes
R_s	Stator resistance
S	Circular sweep of the turbine
T_g	Generator torque
T_t	Aerodynamic torque
T_{em}	Electromagnetic torque
T_f	Damping torque
V	Wind speed [m/s]
λ_{optm}	Optimal speed ratio
ϕ_f	Flux of magnets
ρ	Air density [kJ/kg·K]

REFERENCES

Adelekan, O. A., Ilugbusi, B. S., Adisa, O., Obi, O. C., Awonuga, K. F., Asuzu, O. F., & Ndubuisi, N. L. (2024). Energy transition policies: a global review of shifts towards renewable sources. *Engineering Science & Technology Journal*, *5*(2), 272‑287. https://doi.org/10.51594/estj.v5i2.752.

Ahmadi, M., Poshtan, J., & Poshtan, M. (2012). Modelling squirrel cage induction motors using finite element method. *2012 IEEE International Conference on Intelligent Control, Automatic Detection and High-End Equipment*, 186‑191. https://doi.org/10.1109/ICADE.2012.6330124.

Ashrafzadeh, S. A., Ghadimi, A. A., Jabbari, A., & Miveh, M. R. (2024). Optimal design of a modular axial- flux permanent- magnet synchronous generator for gearless wind turbine applications. *Wind Energy*, *27*(3), 258‑276. https://doi.org/10.1002/we.2887.

Azevedo, I. A., & Barros, L. S. (2021). Comparison of control strategies for squirrel-cage induction generator-based wind energy conversion systems. *2021 14th IEEE International Conference On Industry Applications (INDUSCON)*, São Paulo, Brazil, 790‑796. DOI: 10.1109/INDUSCON51756.2021.9529574.

Barmpatza, A. C. (2023). The neutral voltage difference signal as a means of investigating eccentricity and demagnetization faults in an AFPM synchronous generator. *Machines*, *11*(6), 647. https://doi.org/10.3390/machines11060647.

Bouhafs, L., Tamalouzt, S., & Bouzida, A. (2025). A novel approach to feature extraction from gear condition monitoring signals. *Acta Polytechnica*, *65*(2), 167‑176. https://doi.org/10.14311/AP.2025.65.0167.

Boztaş, A., Demirbaş, O., & Şahin, M. E. (2021). Investigation of vertical axis wind turbines and the design of their components. *Turkish Journal of Electromechanics and Energy*, *6*(2), 64‑72.

Burton, T., Jenkins, N., Sharpe, D., & Bossanyi, E. (2011). *Wind Energy Handbook*. John Wiley & Sons.

Çabuk, A. S., & Üstün, Ö. (2023). Thermal optimization of a radial flux permanent magnet synchronous motor with axial division. *Turkish Journal of Electrical Power and Energy Systems*, *3*(2), 61‑68. https://doi.org/10.5152/tepes.2023.23014.

Esenboğa, B. (2024). Comparative performance analysis of PMSGs using various core materials for wind turbine application. *Osmaniye Korkut Ata Üniversitesi Fen Bilimleri Enstitüsü Dergisi*, *7*(5), 2217‑2231. https://doi.org/10.47495/okufbed.1454674.

Farhan, N. S., Humod, A. T., & Hasan, F. (2021). Field oriented control of AFPMSM for electrical vehicle using adaptive neuro-fuzzy inference system (ANFIS). Eng. Technol. J, 39(10), 1582‑1571. https://doi.org/10.30684/etj.v39i10.1969.

Hölsch, L., Brosch, A., Steckel, R., Braun, T., Wendel, S., Böcker, J., & Wallscheid, O. (2024). Insights and challenges of co-simulation-based optimal pulse pattern evaluation for electric drives. *IEEE Transactions on Energy Conversion*, *39*(3), 2094‑2105. https://doi.org/10.1109/TEC.2024.3374962.

Lakshmi, N. S., Krithik, E. N., Santhoshkumar, V., Santhosh, A. P., & Prabhu, A. (2025). Design and development of PMSM drive controller for electric Go-Kart. Proceedings of the *2*025 International Conference on Advanced Research in Electronics and Communication Systems (ICARECS-2025), 274‑287. DOI: 10.2991/978-94-6463-754-0_25.

Liu, C., Yang, G., Wang, Y., Lei, G., & Zhu, J. (2025). Comparative study of radial, axial and transverse flux generators with hybrid cores for 5 kW wind generator. *Journal of Electrical Engineering & Technology*, *20*(5), 3123‑3134. https://doi.org/10.1007/s42835-025-02231-4.

Mersha, T. K., & Du, C. (2021). Co-simulation and modeling of PMSM based on ANSYS software and Simulink for EVs. *World Electric Vehicle Journal*, *13*(1), 4. https://doi.org/10.3390/wevj13010004.

Şahin, M. E., Sharaf, A. M., Okumuş H. İ. (2012). A novel filter compensation scheme for single phase-self-excited induction generator micro wind generation system. *Scientific Research and Essays*, *7*(34). https://doi.org/10.5897/SRE11.708.

Tabassum, A. A., Cho, H. M., & Mahmud, M. I. (2024). Essential features and torque minimization techniques for brushless direct current motor controllers in electric vehicles. *Energies*, *17*(18), 4562. https://doi.org/10.3390/en17184562.

Veers, P., Bottasso, C. L., Manuel, L., Naughton, J., Pao, L., Paquette, J. et al. (2023). Grand challenges in the design, manufacture, and operation of future wind turbine systems. *Wind Energy Science*, *8*(7), 1071‑1131. https://doi.org/10.5194/wes-8-1071-2023.

Zhu, X., Qi, G., Han, P., Wang, Y., Hua, W., Huang, J., Li, X., & Cui, Y. (2023). Performance analysis of hts armature axial flux magnetic field modulation direct drive wind generator. *IEEE Transactions on Applied Superconductivity*, *33*(5), 1‑8, 5202508. https://doi.org/10.1109/TASC.2023.3266717.